(15) MacDiarmid, A. G.; Yang, L. S.; Huang, W. S.; Humphrey, B. D. *Synth. Met.* **1987**, *18*, 393.
(16) In this paper the terms 2S, 2A, 1S, and 1A, proposed by MacDiarmid et al.,[4] are used for forms of polyaniline.
(17) Furukawa, Y.; Hara, T.; Hyodo, Y.; Harada, I. *Synth. Met.* **1986**, *16*, 189.
(18) This compound is also called *N,N'*-diphenyl-*p*-phenylenediamine and *N,N'*-diphenyl-*p*-benzoquinone diamine and termed QDA in the previous paper.[17]
(19) This compound is also called *N,N'*-diphenyl-*p*-phenylenediimine and *N,N'*-diphenyl-*p*-benzoquinone diimine and termed QDI in the previous paper.[17]
(20) Honzl, J.; Metalová, M. *Tetrahedron* **1969**, *25*, 3641.
(21) Linschitz, H.; Rennert, J.; Korn, T. M. *J. Am. Chem. Soc.* **1954**, *76*, 5839.
(22) Varsányi, G. *Vibrational Spectra of Benzene Derivatives*; Academic Press: New York, 1969.
(23) Lord, R. C.; Marston, A. L.; Miller, F. A. *Spectrochim. Acta* **1957**, *9*, 113.
(24) Cao, Y.; Li, S.; Xue, Z.; Guo, D. *Synth. Met.* **1986**, *16*, 305.
(25) Ohira, M.; Sakai, T.; Takeuchi, M.; Kobayashi, Y.; Tsuji, M. *Synth. Met.* **1987**, *18*, 347.
(26) Ohsaka, T.; Ohnuki, Y.; Oyama, N.; Katagiri, G.; Kamisako, K. *J. Electroanal. Chem. Interfacial Electrochem.* **1984**, *161*, 399.
(27) Nakanishi, K.; Solomon, P. H. *Infrared Absorption Spectroscopy*, 2nd ed.; Holden-Day: San Francisco, 1977.
(28) Nakajima, T.; Harada, M.; Osawa, R.; Kawagoe, T.; Furukawa, Y.; Harada, I., to be published.
(29) MacDiarmid, A. G.; Chiang, J. C.; Richter, A. F.; Epstein, A. J. *Synth. Met.* **1987**, *18*, 285.
(30) Hagiwara, T.; Demura, T.; Iwata, K. *Synth. Met.* **1987**, *18*, 317.
(31) Epstein, A. J.; Ginder, J. M.; Zuo, F.; Bigelow, R. W.; Woo, H.-S.; Tanner, D. B.; Richter, A. F.; Huang, W.-S.; MacDiarmid, A. G. *Synth. Met.* **1987**, *18*, 303.
(32) Nakajima, T.; Kawagoe, T.; Furukawa, Y.; Harada, I., unpublished data.
(33) Perrier-Datin, A.; Lebas, J.-M. *J. Chim. Phys. Phys.-Chim. Biol.* **1972**, *69*, 591.
(34) Wnek, G. E. *Synth. Met.* **1986**, *15*, 213.
(35) Kobayashi, T.; Yoneyama, H.; Tamura, H. *J. Electroanal. Chem. Interfacial Electrochem.* **1984**, *177*, 281.
(36) Huang, W.-S.; Humphrey, B. D.; MacDiarmid, A. G. *J. Chem. Soc., Faraday Trans. 1* **1986**, *82*, 2385.

Static and Dynamic Scattering from Block Copolymeric Ring Molecules

Klaus Huber†

Department of Chemistry, Dartmouth College, Hanover, New Hampshire 03755.
Received September 14, 1987

ABSTRACT: Some conformational properties of diblock Gaussian ring copolymers are investigated. Explicit expressions are derived for the apparent mean-square radius of gyration, the apparent diffusion coefficient, and the angular dependence of the first cumulant of the dynamic structure factor. The results are discussed for rings of different relative block size and varying optical contrast among monomers and solvent.

Introduction

Various theoretical effects have been undertaken to describe the scattering behavior of linear[1-3] and branched[4,5] copolymers. The technique of anionic polymerization offers a powerful method to synthesize well-defined block copolymers of various structures.[6-8] Since the synthesis of ring polymers by anionic polymerization is now well developed,[9-11] extension of the technique to block copolymeric rings can be expected in the near future. In order perhaps to encourage such development, some scattering properties of diblock ring polymers are considered here.

The properties discussed are the mean-square radius of gyration, the particle scattering function, the diffusion coefficient, and the first cumulant of the dynamic structure factor. Two particular questions are investigated in some detail: (i) the influence of the ring constraint on homopolymeric parts of the molecules; (ii) the scattering behavior of chemically heterogeneous ring polymers in comparison to the corresponding homopolymers.

The calculation of the particle scattering function as well as of the first cumulant from block copolymeric rings involves some integrations which could only be treated numerically. These were performed by using the Dartmouth IMSL programs DCADRE, DBLIN, and DMLIN.

Model

The polymer model used is based on the Gaussian distribution of distances between any two monomers of the same polymer. We consider rings which consist of two blocks (A and B) with monomers differing in one or more of the following properties: length of a monomeric unit, hydrodynamic friction coefficient (ζ), refractive index increment (ν), and weight of the monomeric unit (M_0). The number of monomers in block A is n, each of length a; block B contains m monomers, all of length b. We write

$$N = n + m \tag{1}$$

for the total number of monomers in the ring. Thermodynamic interactions between chemically different monomers are not taken into account. Under this assumption, the scattering behavior from monodisperse copolymers can be described by[1-3]

$$S(q,t) = \nu^{-2}\sum_{l=1}^{N}\sum_{j=1}^{N}\nu_l\nu_j M_{0_l}M_{0_j}\langle\exp(i\mathbf{q}\cdot\mathbf{r}_{lj}(t))\rangle \tag{2}$$

where $S(q,t)$ is the dynamic structure factor, $\mathbf{r}_{l_j}(t)$ the distance vector between the location of monomer l at time 0 and monomer j at time t, $\mathbf{q}$ the scattering vector, M the overall molecular weight, and ν the average refractive index increment of the copolymer in solution.

$$\nu = \sum_k w_k\nu_k \tag{3}$$

Here w_k is the weight fraction and ν_k the refractive index increment of the kth component.

The initial part of the dynamic structure factor, which is a decaying function of t, can be characterized by the first cumulant,

$$\Gamma = \lim_{t\to 0}[-\partial \ln S(q,t)/\partial t] \tag{4}$$

†Present address: Institut für Makromolekulare Chemie, der Universität Freiburg, Stefan-Meier-Str. 31, D-7800 Freiburg, FRG.

0024-9297/88/2221-1305$01.50/0

If t is set equal to zero, eq 2 corresponds to the static scattering behavior $S(q,0)$ which is usually represented by the normalized particle scattering function:

$$P(q) = S(q,0)/S(0,0) \tag{5}$$

For convenience, we define

$$\xi_a = \nu_a M_{0_a} \tag{6a}$$

$$\xi_b = \nu_b M_{0_b} \tag{6b}$$

where a and b indicate blocks A and B. As can be seen from eq 2, the apparent molecular weight of the copolymer is $M_{app} = \lim_{q\to 0} S(q)/M$. If each copolymer molecule has identical composition and degree of polymerization, M_{app} is equal[1,3] to the true M, as for all the examples treated in this paper, and then

$$M_{app}M = M^2 = (n^2\xi_a^2 + 2mn\xi_a\xi_b + m^2\xi_b^2)/\nu^2 \tag{7}$$

We first recall some existing results on homopolymeric Gaussian rings. The mean-square radius of gyration is[12,13]

$$\langle S^2\rangle = Na^2/12 \tag{8}$$

with N the total number of monomers of root mean squared length a. This is exactly half the value for the corresponding linear Gaussian chain. The particle scattering function was derived by Casassa[14] to be

$$P(q) = (2/\langle S^2\rangle q^2)^{1/2} D[(\langle S^2\rangle q^2/2)^{1/2}] \tag{9}$$

Here

$$D\{X\} = \exp(-X^2)\int_0^x \exp(t^2)\,dt \tag{10}$$

is the Dawson integral, which is tabulated,[15] and $q = (4\pi/\lambda)\sin(\theta/2)$ is the absolute value of the scattering vector.

The dynamic scattering behavior of homopolymeric rings was treated more recently by Burchard and Schmidt.[16] Their equation for the first cumulant is

$$\Gamma/q^2 = k_B T\left[(1/\zeta N) + (q/6\pi^{3/2}\eta_0 N)\int_1^N I(X)\,ds\right]\Big/ P(q) \tag{11a}$$

where k_B is the Boltzmann constant, T the temperature, η_0 the solvent viscosity, ζ the friction coefficient of a monomer, and

$$X^2 = q^2\mu_s/6 \tag{11b}$$

$$4I(X)/3 = (2X^{-2} + X^{-4})D(X) - X^{-3} \tag{11c}$$

$$\mu_s = a^2 s(1 - s/N) \tag{11d}$$

where s indicates the number of monomers forming a subchain within the ring.

The statistics of homopolymeric Gaussian rings is described by the probability distribution

$$P(r_s) = (3/2\pi\mu_s)^{3/2}\exp(-3r_s^2/2\mu_s) \tag{12}$$

In the case of block rings the corresponding equation is

$$P(r_{st}) = (3/2\pi\mu_{st})^{3/2}\exp(-3r_{st}^2/2\mu_{st}) \tag{13}$$

with

$$\mu_{st} = (sa^2 + tb^2)[1 - (sa^2 + tb^2)/(na^2 + mb^2)] \tag{14}$$

where s and t are the numbers of monomers from block A and B, respectively, which form the subchain of end-to-end distance r_{st}. Necessarily $0 \le s \le n$ and $0 \le t \le m$. Equation 2 is based on double sums over all possible pair combinations of monomers. The derivations carried out in the following sections exhibit the common feature that the pair combinations can be subdivided into three different types: (i) both monomers belong to block A; (ii) both monomers belong to block B; (iii) each monomer belongs to a different block.

Static Scattering

In order to calculate the particle scattering function, the starting equation is eq 2 at $t = 0$. After subdivision of the double sum the expression contains three terms.

$$P(q) = [S_a(q) + S_b(q) + S_{ab}(q)]/M^2 \tag{15}$$

where

$$S_a(q) = \xi_a^2\nu^{-2}[2\sum_{s=0}^{n-1}(n - s)\exp[-(q^2\mu_s/6)] - n] \tag{16a}$$

$$S_b(q) = \xi_b^2\nu^{-2}[2\sum_{t=0}^{m-1}(m - t)\exp[-(q^2\mu_t/6)] - m] \tag{16b}$$

$$S_{ab}(q) = \xi_a\xi_b\nu^{-2}[2\sum_{t=1}^{m}\sum_{s=0}^{n}\exp[-(q^2\mu_{st}/6)]] \tag{16c}$$

Equation 16 results immediately from averaging $\exp(-i\mathbf{q}\cdot\mathbf{r}_{ij})$ over all possible orientations and distances. If the sums in eq 16 are changed into integrals and we define

$$A = na^2 + mb^2 \tag{17}$$

then eq 15 reads

$$P(q) = 2\exp(-Aq^2/24)\nu^{-2}\Big[\xi_a^2\int_0^n (n - s)\times \exp[q^2(sa^2 - A/2)^2/6A]\,ds + \xi_b^2\int_0^m (m - t)\exp[q^2(tb^2 - A/2)^2/6A]\,dt + \xi_a\xi_b\int_0^n ds\int_0^m dt\exp[q^2(sa^2 + tb^2 - A/2)^2/6A]\Big]\Big/ M^2 \tag{18}$$

which is the particle scattering function of a ring-shaped block polymer. If we make ξ_a equal to ξ_b and a equal to b, eq 18 becomes identical with eq 9 for homopolymeric ring molecules.

As in the case of the homopolymeric ring, $P(q)$ in eq 18 can only be expressed in terms of the Dawson integral. However, it is possible to get an explicit expression for the apparent mean-square radius of gyration, since

$$\langle S^2\rangle_{app} = -\lim_{q\to 0} 3\,dP(q)/d(q^2) \tag{19}$$

We find

$$\langle S^2\rangle_{app} = \frac{1}{12AM^2\nu^2}[n^2\xi_a^2(n^2a^4 + 2na^2mb^2) + m^2\xi_b^2(m^2b^4 + 2mb^2na^2) + 2mn\xi_a\xi_b(n^2a^4 + 3na^2mb^2 + m^2b^4)] \tag{20}$$

Again it can be shown easily that eq 20 leads to eq 8 if $\xi_a = \xi_b$ and $a = b$.

Dynamic Scattering

According to Akcasu and Gurol,[17] the first cumulant $\Gamma(q^2)$ in general can be calculated via

$$\Gamma(q^2) = \frac{\sum_{i=1}^{N}\sum_{j=1}^{N}\xi_i\xi_j\langle(\mathbf{q}\cdot\mathbf{D}_{ij}\cdot\mathbf{q})\exp(i\mathbf{q}\cdot\mathbf{r}_{ij})\rangle}{\nu^2 S(q,0)} \tag{21}$$

where

$$\mathbf{D}_{lj} = k_B T\left[\frac{\delta_{lj}}{\zeta}\mathbf{I} + \frac{1-\delta_{lj}}{8\pi\eta_0 \mathbf{r}_{lj}}\left(\mathbf{I} - \frac{\mathbf{r}_{lj}\mathbf{r}_{lj}}{\mathbf{r}_{lj}^2}\right)\right] \quad (22)$$

is the diffusion tensor with $\mathbf{I}$ the unit matrix. The hydrodynamic interactions in eq 21 are not preaveraged. Subdivision of the double sum in eq 21, subsequent averaging over all orientations and distances, and finally a change to integrals yield

$$\Gamma_a = (k_B T q^2/\nu^2 M^2) \times \left[\xi_a^2 n/\zeta_a + 2q\xi_a^2\kappa\int_1^n (n-s)I(X)\,ds\right]\Big/P(q) \quad (23a)$$

with $X^2 = \mu_s q^2/6$,

$$\Gamma_b = (k_B T q^2/\nu^2 M^2) \times \left[\xi_b^2 m/\zeta_b + 2q\xi_b^2\kappa\int_1^m (m-t)I(X)\,dt\right]\Big/P(q) \quad (23b)$$

with $X^2 = \mu_t q^2/6$,

$$\Gamma_{ab} = \left[2q^2\frac{\xi_a\xi_b k_B T}{\nu^2 M^2}\kappa\int_0^m dt\int_0^n ds\, I(X)\right]\Big/P(q) \quad (23c)$$

with $X^2 = \mu_{st} q^2/6$. The constant κ is defined as

$$\kappa = (1/6\pi^{3/2}\eta_0) \quad (24)$$

and the indices a, b, and ab indicate the type of pair combinations included by the corresponding terms. The apparent first cumulant Γ_{app} for the block copolymeric ring is just the sum of eq 23a through 23c. Because $I(X)$ contains the Dawson integral (see eq 11c), $\Gamma_{app}(q^2)$ can only be calculated numerically. But, as in the case of $\langle S^2\rangle_{app}$, the limiting behavior at small q gives an exact expression for the apparent diffusion coefficient

$$D_{app} = \lim_{q\to 0}(\Gamma_{app}/q^2) \quad (25)$$

as well as for the initial q^2 dependence of Γ_{app}

$$\lim_{q^2\to 0}\frac{\partial(\Gamma_{app}/q^2)}{\partial q^2} = C_{app}\langle S^2\rangle_{app} D_{app} \quad (26)$$

Equation 26 results from a series expansion of Γ_{app}/q^2 around $q^2 = 0$.

$$\Gamma_{app} = D_{app}(1 + C_{app}\langle S^2\rangle_{app} q^2 + ...) \quad (27)$$

If we take the limit $q \to 0$ in eq 23, X becomes 0 and $I(X)$ approaches $^4/_3$ which leads to

$$D_{app} = \frac{k_B T}{\nu^2 M^2}\left[\frac{n\xi_a^2}{\zeta_a} + \frac{m\xi_b^2}{\zeta_b} + \frac{2}{6^{1/2}\pi^{3/2}\eta_0}(\xi_a^2 I_a + \xi_b^2 I_b + \xi_a\xi_b I_{ab})\right] \quad (28)$$

The expressions for I_a, I_b, and I_{ab} are rather lengthy and are therefore given separately in the Appendix.

In order to investigate the initial angular dependence of Γ_{app}/q^2, the Dawson integrals in eq 23 were expanded in powers of q^2 around $q^2 = 0$. Subsequent integration in eq 23 finally leads to a relationship of the type of eq 27, where

$$C_{app} = 1/3 + \frac{8\kappa}{5\nu^2 M^2 6^{1/2}}(\xi_a^2 IC_a + \xi_b^2 IC_b - \xi_a\xi_b IC_{ab})/(D_{app}\langle S^2\rangle_{app}) \quad (29)$$

Again, the explicit representation of IC_a, IC_b, and IC_{ab} is offered in the Appendix. If a equals b, ζ_a equals ζ_b and ξ_a equals ξ_b; D_{app} and C_{app} reduce to the relationships given by Burchard and Schmidt[16] for hompolymeric rings.

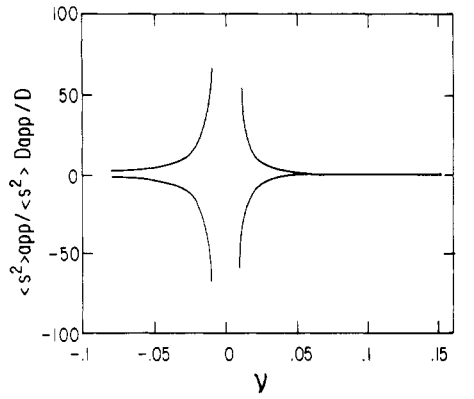

Figure 1. Ratio of apparent to true mean-square radii of gyration (lower curve) and diffusion coefficients (upper curve) plotted versus ν. $\langle S^2\rangle$ and D indicate the case where $\xi_a = \xi_b$.

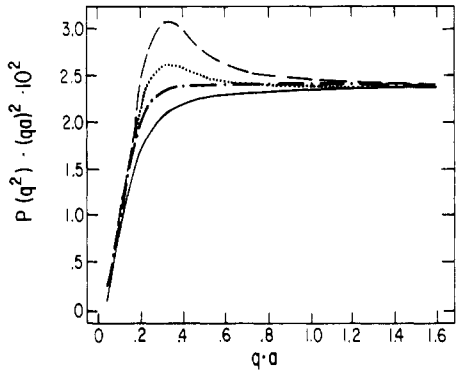

Figure 2. Kratky plots of particle scattering functions: (---) A block, $n = m = 500$, $\nu_b = 0$; (···) A block, $n = 500$, $m = 135$, $\nu_b = 0$; (--) ring homopolymer, $N = 500$; (—) homopolymeric linear chain, $N = 500$.

Results and Discussion

Behavior at Small q. Equation 20 gives an apparent geometric size, the radius of gyration, which is determined by the initial slope of the particle scattering function. Another parameter with the dimension of a length is the hydrodynamic radius; it is proportional to the reciprocal of D_{app} and therefore calculated from Γ_{app} at $q = 0$.

Figure 1 represents the ratio of the apparent mean-square radius of gyration to the real one, together with the corresponding ratio for the apparent diffusion coefficient. Real values of $\langle S^2\rangle$ and Γ are found by making ξ the same in both blocks. If ν_a cancels ν_b, the apparent mean-square radius of gyration goes to minus infinity and the apparent hydrodynamic radius approaches zero which is simply because the denominator in eq 20 and 23 becomes zero. This behavior is a general feature of copolymers, independent of spatial structure.

Special interest attaches to the case where only one block of the ring is "visible" by scattering experiments; e.g., $\nu_b = 0$. It is of interest now to change the size of one block relative to the other one. This is done in Figures 2 and 3 by varying the number of monomers in the invisible block B at constant n. With decreasing m, both the static and dynamic scattering behavior of block A shows a transition from that of a linear chain to that of a ring. If $n \le m$, the maximum of the scattering function in the Kratky plot disappears. This maximum value is a typical feature for molecules with a high segment density as is the case for homopolymeric stars[18] and rings.[16]

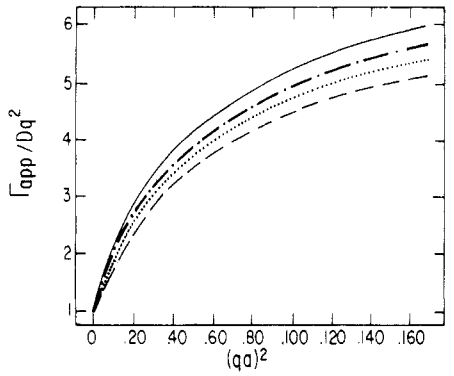

Figure 3. Reduced first cumulant, Γ_{app}/Dq^2, where D is the true translational diffusion coefficient. The curves correspond to the same structures as in Figure 2.

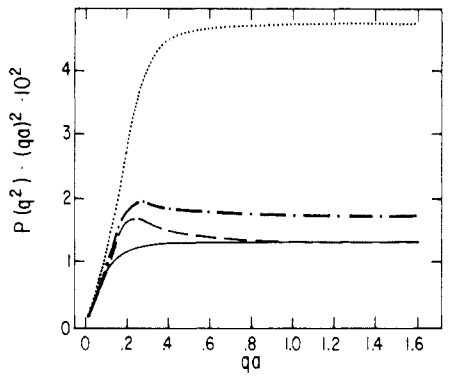

Figure 4. Kratky plots of particle scattering functions. All ring chains have $n = m = 500$. (---) $\nu_a = 0.1$, $\nu_b = 0.025$; (···) $\nu_a = 0.1$, $\nu_b = -0.025$; (--) $\nu_a = \nu_b = 0.1$; (—) homopolymeric linear chain.

An equivalent way to change the relative sizes of the two blocks is to vary the lengths of the monomeric units. For example, the number of monomers in the two blocks could be kept constant, with $m = n$, and then the length b could be varied from values much larger than a to values much lower than a. Since only the combinations na^2 and mb^2 occur in the equations, as is necessarily true for strictly Gaussian models, the visible block A again changes its behavior from a regular linear chain to a ring.

$\nu_a \neq \nu_b$. In this case a wide variety of scattering patterns can be covered by changing ν_b within the limits $\nu_a \geq \nu_b \geq -\nu_a$ and simultaneously changing the relative amounts of monomers or the monomeric lengths within the two blocks. In this paper we confine ourselves to the case, where both blocks are equal in size; i.e., $a = b$ and $n = m$. The refractive index increment of block A is taken equal to 0.100.

Figure 4 represents the particle scattering function of two rings with $\nu_b = 0.025$ and -0.025 in comparison to the homopolymeric ring and the linear chain at the same total number of segments. Figure 5 represents the corresponding situation in a dynamic scattering experiment. If ν_b is increased, the curves resemble more and more that of a homopolymeric ring. The maximum value in the Kratky plot of the scattering function appears only for $\nu_b > 0$.

In principle, it should be possible to test these predictions by static and dynamic light scattering. However, it is not at present sure that ring polymers can be synthesized which are large enough to display an extended angular dependence of $P(q)$ or $\Gamma(q)$, and supplementing neutron scattering experiments may be required. In the latter case, the contrast which is necessary for a scattering experiment is provided by differing scattering lengths for neutrons, instead of the refractive index increments. This only leads

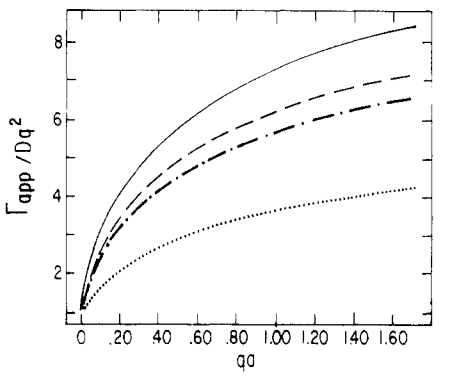

Figure 5. Reduced first cumulant; the curves correspond to the same structures as in Figure 4.

to modifications in eq 2, 3, 6, and 7. All equations otherwise remain the same.

Acknowledgment. I thank the Alexander von Humboldt-Stiftung for a Feodor Lynen Research Fellowship, during the period of which this work was done. I express my gratitude to Professor W. H. Stockmayer for drawing attention to this problem and for his frequent advice. This work was also supported by the National Science Foundation, under Grant DMR 860 8633, Division of Materials Research, Polymers Program.

Appendix

In eq 28

$$I_a = (A^{1/2}/a^4)[(B/2)[\arcsin(1 - 2a^2/A) - \arcsin(-B/A)] + (nmb^2a^2)^{1/2} - (Aa^2 - a^4)^{1/2}]$$

$$I_b = (A^{1/2}/b^4)[(-B/2)[\arcsin(1 - 2b^2/A) - \arcsin(B/A)] + (nma^2b^2)^{1/2} - (Ab^2 - b^4)^{1/2}]$$

$$I_{ab} = (A^{1/2}/b^2a^2) \times [-B \arcsin(B/A) + (A) \arcsin(1) - 2(nma^2b^2)^{1/2}] \quad \text{(A1)}$$

In eq 29

$$IC_a = a[[-(nmb^2)^{3/2} + (A - a^2)^{3/2}]/[A^{1/2}a^23] - (B/16a^2)[2(B/a^2)(nmb^2/A)^{1/2} - (A^{3/2}/a^3) \arcsin(-B/A)] + (B/16a^2)[2(2 - A/a^2) \times (1 - a^2/A)^{1/2} - (A^{3/2}/a^3) \arcsin(1 - 2a^2/A)]]$$

$$IC_b = b[[-(nma^2)^{3/2} + (A - b^2)^{3/2}]/[A^{1/2}b^23] + (B/16b^2)[-2(B/b^2)(nma^2/A)^{1/2} - (A^{3/2}/b^3) \arcsin(B/A)] - (B/16b^2)[2(2 - A/b^2) \times (1 - b^2/A)^{1/2} - (A^{3/2}/b^3) \arcsin(1 - 2b^2/A)]]$$

$$IC_{ab} = +(1/a^2b^2A^{1/2})(nma^2b^2)^{3/2}/3 + (A/8)I_{ab} \quad \text{(A2)}$$

where $A = na^2 + mb^2$ and $B = na^2 - mb^2$.

The quantities in eq A1 are of $\mathcal{O}(N^{3/2})$ and those in eq A2 of $\mathcal{O}(N^{5/2})$ for large N. We have not troubled to perform expansions of the above equations, since the computations are not difficult in any case.

References and Notes

(1) Stockmayer, W. H.; Moore, L. D.; Fixman, M.; Epstein, B. N. *J. Polym. Sci.* **1955**, *16*, 517.
(2) Bushuk, W.; Benoit, H. *Can. J. Chem.* **1958**, *36*, 1616.
(3) Benoit, H.; Wippler, C. *J. Chim. Phys. Phys.-Chim. Biol.* **1960**, *57*, 524.
(4) Gordon, M.; Malcolm, G. N.; Butler, D. S. *Proc. R. Soc. London, A* **1966**, *256*, 29.
(5) Burchard, W.; Kajiwara, K.; Nerger, D.; Stockmayer, W. H. *Macromolecules* **1984**, *17*, 222.
(6) (a) Szwarc, M.; Levy, M.; Milkovich, R. *J. Am. Chem. Soc.* **1956**, *78*, 2656. (b) Szwarc, M. *Carbanions, Living Polymers*

and Electron Transfer Processes; Interscience: New York, 1968.
(7) Gallot, Y.; Rempp, P.; Parrod, J. J. Polym. Sci., Polym. Lett. Ed. 1963, 1, 329.
(8) Nguyen, A. B.; Hadjichristidis, N.; Fetters, L. J. Macromolecules 1986, 19, 768.
(9) Hild, G.; Kohler, E.; Rempp, P. Eur. Polym. J. 1980, 16, 525.
(10) Geiser, D.; Höcker, H. Macromolecules 1980, 13, 653.
(11) Roovers, J.; Toporowski, P. M. Macromolecules 1983, 16, 843.
(12) Kramers, H. A. J. Chem. Phys. 1946, 14, 415.
(13) Zimm, B.; Stockmayer, W. H. J. Chem. Phys. 1949, 17, 1301.
(14) Casassa, E. F. J. Polym. Sci., Part A 1965, 3, 605.
(15) Abramowitz, M.; Stegun, I. A. Handbook of Mathematical Functions; Dover: New York, 1970; p 319, Table 7.5.
(16) Burchard, W.; Schmidt, M. Polymer 1980, 21, 745.
(17) Akcasu, A. Z.; Gurol, H. J. Polym. Sci. 1976, 14, 1.
(18) Burchard, W. Macromolecules 1977, 10, 919.

Microstructure and Property Changes Accompanying Hard-Segment Crystallization in Block Copoly(ether–ester) Elastomers

Janis Castles Stevenson and Stuart L. Cooper*

Department of Chemical Engineering, University of Wisconsin—Madison, Madison, Wisconsin 53706. *Received August 25, 1987*

ABSTRACT: Hard-segment crystallization is a primary factor governing the properties of copoly(ether–ester) elastomers composed of poly(tetramethylene oxide) soft segments and poly(tetramethylene terephthalate) and/or poly(tetramethylene isophthalate) hard segments. Differential scanning calorimetry, tensile testing, and small-angle X-ray scattering have been used to follow the structure and property changes occurring during the room-temperature crystallization of copoly(ether–ester) elastomers in which poly(tetramethylene isophthalate) is the major hard-segment component. The measurements show that crystallization leads to significant improvements in tensile properties, particularly as the sample crystalline weight fraction increases from 0.05 to 0.10. These improvements have been attributed to hard-domain development from a dispersion of tie points that act as isolated entities to a network of cross-links that function collectively during deformation.

I. Introduction

Thermoplastic elastomers are materials that exhibit a unique combination of strength, flexibility, and processability due to their phase-separated microstructure. The elastomers are copolymers composed of two different types of segments, commonly referred to as "soft" and "hard" segments. The soft segments are derived from oligomers having a low glass transition temperature and are viscous at elastomer service temperatures, imparting flexibility to the material. Interactions between the hard segments lead to phase separation in which hard segment rich microdomains are formed that serve as physical cross links, contributing to the strength and dimensional stability of the material. Phase separation may involve hard segment vitrification, crystallization, hydrogen bonding, and/or ionic clustering.

One system in which hard-segment crystallization is particularly important is the copoly(ether–ester) elastomer based on soft segments of poly(tetramethylene oxide) (PTMO) and hard segments of poly(tetramethylene terephthalate) (PTMT) and/or poly(tetramethylene isophthalate) (PTMI) as illustrated in Figure 1. These copolymers have found extensive use in extrusion and molding resins for a wide variety of products. The morphology of such elastomers has been described in terms of a two-phase structure composed of crystalline hard domains relatively pure in hard segments and amorphous soft domains formed by a mixture of hard and soft segments.[1] The thermal and mechanical properties of the materials have been shown to vary with the fraction and type of hard-segment crystallinity present.[2] In order to understand such property variations, the underlying changes in polymer microstructure must be examined. In the present study, small-angle X-ray scattering measurements have been combined with differential scanning calorimetry and tensile measurements to elucidate the microstructure and property changes associated with hard-segment crystallization.

The crystallization rates of the copoly(ether–ester) elastomers depend upon which type of hard segment is the major crystallizing component. Copoly(ether–esters) in which PTMT is predominant crystallize rapidly upon cooling from the melt to room temperature; a substantial fraction of the crystallization occurs during cooling, even at cooling rates of 160 °C/min.[3] This leads to high production rates in manufacturing and is one reason why the commercial elastomers, marketed as Hytrel, contain primarily PTMT hard segments. However, the high crystallization rate makes it difficult to study the associated structure and property changes as they occur. In copoly(ether–esters) in which PTMI is the major hard-segment component, only a small amount of crystallization, if any, occurs during rapid cooling from the melt to room temperature. The samples are essentially transparent when removed from the mold, but, over a period of hours at room temperature, they gradually cloud with white specks and streaks and may eventually become entirely opaque. Simple probes such as flexing, stretching, or cutting the films at different degrees of opacity reveal remarkable changes in the properties of the copolymers. The crystallization rate is slow enough to allow these changes to be chronicled and quantified by using thermal, mechanical, and structural analysis techniques. On the basis of this characteristic, PTMI-rich copolyether–esters have been selected for this study of hard-segment crystallization.

II. Experimental Section

A. Materials. The copoly(ether–esters) used in this study were synthesized by melt transesterification of dimethyl terephthalate, dimethyl isophthalate, 1,4-butanediol, and poly(tetramethylene ether) glycol following a procedure similar to that described by Witsiepe.[4] A glycol with a number average molecular weight of approximately 1000 was used. Soft-segment crystallization is generally observed only for copolymers derived from glycols of 2000 MW or greater;[5,6] crystallization in the present materials was thus limited to the hard segments. The resultant segmented copolymers contain alternating soft-segment blocks

0024-9297/88/2221-1309$01.50/0